LU TP 99-05
February 1999

A Parametrization for $K^+ \to \pi^+\pi^- e^+\nu$.[†]

Gabriel Amorós[a,b] **and Johan Bijnens**[a]

[a] Department of Theoretical Physics 2, Lund University
Sölvegatan 14A, S 22362 Lund, Sweden

[b] Department of Physics, P.O. Box 9
FIN-00014 University of Helsinki, Finland

Abstract

We discuss various models and Chiral Perturbation Theory results for the K_{l4} form factors F and G. We check in how much a simple parametrization with a few parameters can be used to extract information from experiment.

[†]Work supported in part by TMR, EC-Contract No. ERBFMRX-CT980169 (EURODAΦNE).

1 Introduction

In this note we give a simple parametrization and behaviour with few kinematical variables of the form factors contributing to the decay $K^+ \to \pi^+\pi^- e^+\nu$.

The interest of this work resides in the new measurements of $K \to \pi\pi\ell\nu$ (K_{l4}) to be obtained with new facilities in the inmediate future. The increase in the number of events obtained will give more information about the dependence with the kinematical variables, generalizing and improving the previous and old results [1]. This decay will be a major test of the consistency of the Chiral Perturbation Theory (CHPT), comparing the prediction of some $O(p^4)$ constants of the chiral expansion with the values given by other processes. Even more, this decay is expected to be the best one for a precise determination of the isoscalar $\pi\pi$ S-wave phase shift near threshold which will allow comparing CHPT and other approaches to chiral symmetry breaking. A review of the CHPT results can be found in [2] and references therein.

One of the main results from the previous experiment is the observation of dependence on the energy of the dipion system (s_π). It was consistent with a linear dependence for all the form factors and with the same slope. The contribution from other kinematical variables was not considered. However, as we will see later, the expected variations of the form factors on the energy of the leptonic pair (s_ℓ) and on the $\cos\theta_\pi$, is on the same level as the errors in the previous experiment and will probably become important for the next generation of experiments. In [1] the form factors were fitted with a linear dependence only and the same slope for all form factors. The purpose of this note is to examine various theoretical expectations and check how well a simple extension of this parametrization performs. This will allow then an improved extraction of the $\pi\pi$ phase shifts from the data.

Papers using CHPT and extensions for K_{l4} are [3] and [4]. A review of early work is [5]. An alternative method to extract $\pi\pi$ phases is described in [6, 7] and references therein but it does not allow to use the full experimental information as much as our parametrization allows.

The paper is divided as follows: we introduce the form factors in Sect. 2. We then discuss the singularities that appear in the various cuts in Sect. 3. In Sect. 4 we study two different models for inclusion of resonances, in Sect. 5 CHPT at one loop and with inclusion of part of the p^6 effects in Sect. 6. We then discuss also some unitarization effects and finally the H form factor as well. Sect. 9 contains our proposal for the parametrization of the form factors. The last section contains our conclusions.

2 Form Factors

The decay $K^+(p) \to \pi^+(p_1)\pi^-(p_2)e^+(p_\ell)\nu(p_\nu)$ is given by the amplitude

$$T = \frac{G_F}{\sqrt{2}} V_{us}^\star \bar{u}(p_\nu)\gamma_\mu(1-\gamma_5)v(p_\ell)(V^\mu - A^\mu) \tag{1}$$

where V^μ and A^μ are parametrized in terms of four form factors:

$$\begin{aligned} V_\mu &= -\frac{H}{M_K^3}\epsilon_{\mu\nu\rho\sigma}L^\nu P^\rho Q^\sigma \ , \\ A_\mu &= -i\frac{1}{M_K}\left[P_\mu F + Q_\mu G + L_\mu R\right] \end{aligned} \tag{2}$$

with

$$P = p_1 + p_2 \ , \ Q = p_1 - p_2 \ , \ L = p_\ell + p_\nu \ , \ N = p_\ell - p_\nu \ . \tag{3}$$

and $\epsilon_{0123} = 1$. $\bar{u}$ and v are the lepton Dirac spinors and G_F is the Fermi constant.

In this work we consider the theoretical predictions for the dependence of these form factors F, G and H, with the kinematical variables $s_\pi = (p_1 + p_2)^2$, $s_\ell = (p_\ell + p_\nu)^2$ and $\cos\theta_\pi$ (θ_π is the angle of the π^+ in the $\pi\pi$ system respect to the dipion line of flight). The R-form factor is negligible in decays with an electron in the final state and we will not discuss it.

The relation between form factors and the width can be found in several references [2, 3, 6].

The main objective of this paper is to check in the existing models and calculations in how much simple parametrizations of F, G and H are sufficient. We will basically check if linear dependence on s_π, s_ℓ and $\cos\theta_\pi$ is sufficient or not.

3 Cut Structure

One indication that a constant or a linear structure is enough to describe a given form factor is, how far the masses of the possible intermediate states are from the physical domain. This is done by looking at the states contributing to the various cuts. The possible cuts with strong interaction intermediate states are shown in Fig. 1. We discuss now the cuts in order of the figure.

3.1 Cut (a)

The strong interaction intermediate states that can couple here are in order of their mass: K, $K\pi$, K^*, $K\pi\pi$, K_0, K_1,....

The K and K_0 intermediate states can only contribute to the form factor R which is negligible in this decay. The $K\pi$ and K^* intermediate state are vector

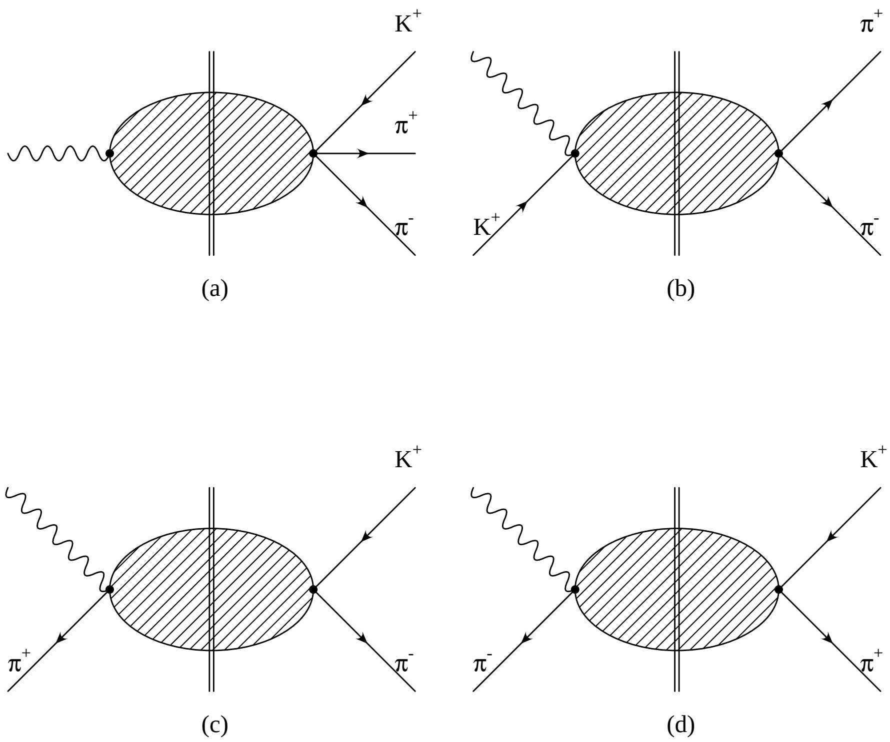

Figure 1: The possible cuts in the decay $K^+ \to \pi^+\pi^-e^+\nu$. The double line is the cut. The wiggly line is the weak current.

states and only contribute to the form factor H. Their effect has been estimated for $K\pi$ by one-loop CHPT and for the K^* by a VMD estimate using the hidden gauge vector model in [8]. There was in effect a large cancellation between the two effects leading to a rather constant form factor across the relevant phasespace. A linear aproximation for both amplitudes separately should in any case be sufficient because the relevant momentum, s_ℓ is far from the thresholds.

The $K\pi\pi$ has a threshold of about 0.765 GeV which is rather far from the physical region which ends at about 0.225 GeV. In addition in CHPT this only starts at the p^6 level. There are two K_1 resonances, one at 1.27 GeV and one at 1.4 GeV. Both are again rather far from the physical region so we expect that their effect will also be small and certainly describable by at most a linear function of s_ℓ.

If one checks the contribution of the axials of [9] we also notice that the axial-vectors only start contributing to this process at order p^6.

In conclusion, we expect the effects of this cut for K_{e4} decays to be linear and fairly small.

3.2 Cut (b)

Here the possible intermediate states are in order of mass again: $\pi\pi$, ρ, f_0,.... The $\pi\pi$ intermediate state is in fact one of the major reasons to study this decay in order to learn more about $\pi\pi$ phase shifts. The cut here is in the physical region for this decay. The effects of $\pi\pi$ final state rescattering will be discussed later, see also [2, 3].

The effects of the ρ are confined mainly to the form factor G. There is a very small curvature in G due to this intermediate state visible in estimates of its effect, although in the region with sufficient data it is rather small. See section 4 for its effect.

3.3 Cut (c)

This channel has charge 2 and has thus no resonance enhancement. The relevant intermediate state is mainly $K\pi$ and this also has a small phase shift in the relevant channel. We thus expect it to be well described by oneloop CHPT.

3.4 Cut (d)

Possible intermediate states here are: $K\pi$, K^*, K_0,.... The relevant variable in this channel is t and it is fairly far away from the threshold. Its effects are thus expected to be well described by a linear function in t, or linear in s_ℓ and $\cos\theta_\pi$. Nonlinear effects on s_ℓ are at most of order $s_\ell^2/m_{K\pi}^4$ which is about 1%. Actual estimates from CHPT at one-loop and various models confirm this expectation.

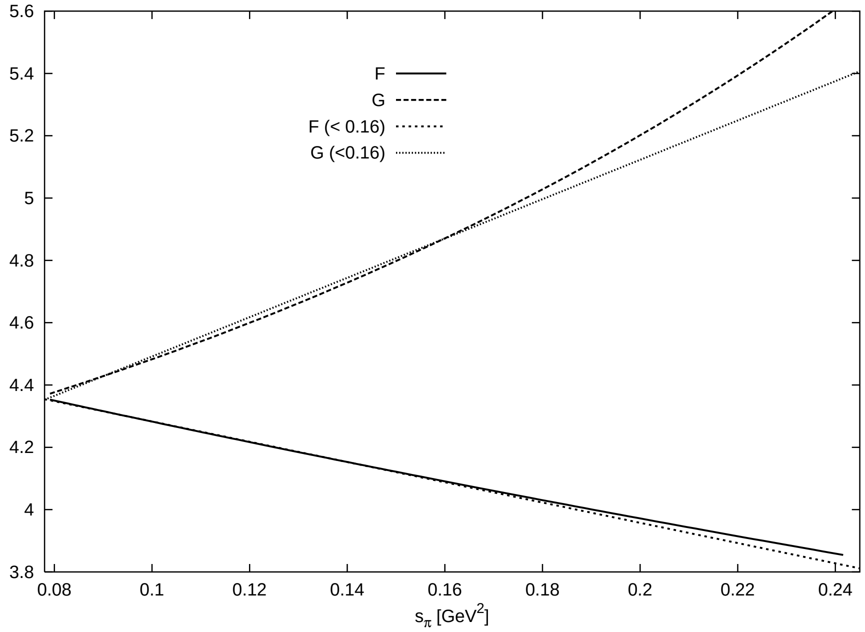

Figure 2: The form factor F and G of the model of Ref. [10] as a function of s_π at $\cos\theta_\pi = s_\ell = 0$.

3.5 Other singularities

In addition to the above real singularities there are also kinematical singularities present in the various quantities. An example of this is the singularities present in the partial waves for $\mathrm{Re}\, s_\pi \leq 0$. These follow because the values of t can become larger than $m_K + m_\pi$ for some values of $\cos\theta_\pi$ and s_ℓ.

4 Resonances

4.1 Resonances in a vector–axial-vector dominance model

In this section we use the model of Ref. [10] for τ decays. Basically this model takes vector and axial-vector mesons and writes the amplitude such that in the low-energy limit all constraints from chiral symmetry are satisfied. In all channels contributions from the two lowest channels are included and the meson propagators are described by Breit-Wigner functions including a s-dependent width.

In Fig. 2 we have shown the F and G form factors of this model as a function of s_π for $\cos\theta_\pi = s_\ell = 0$. In accordance with the discussion in Sect. 3 we see that there is very little curvature. The curvature visible in G is due to the ρ-pole in this model. We have checked this by setting $m_\rho = 1.37$ GeV in the model and

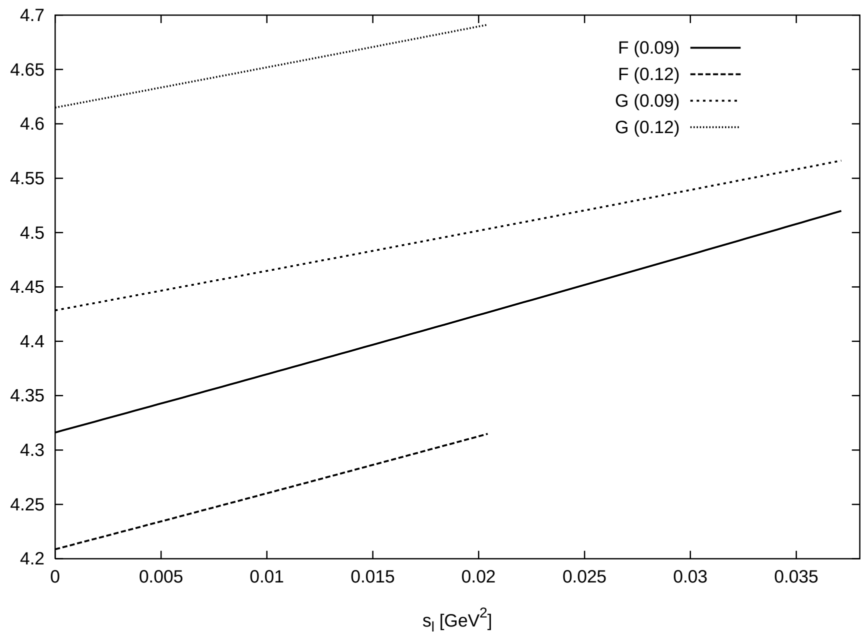

Figure 3: The form factor F and G of the model of Ref. [10] as a function of s_ℓ at $\cos\theta_\pi = 0$ and for $\sqrt{s_\pi} = 0.3$ GeV and $\sqrt{s_\pi} = 0.35$ GeV.

then all curvature disappears. Experimentally there are very few events[1] above $s_\pi = 0.16$ GeV^2 or $E_{\pi\pi} \leq 0.4$ GeV. In the figure the fits linear in s_π to the model curves below this energy are also shown. As can be seen the linear approximation is in the relevant region quite sufficient as an approximation to this model.

Let us now turn to the s_ℓ dependence within this model. In Fig. 3 the form factors F and G are plotted for two values of s_π. These values are in the region where accurate data can be expected. The lines are only plotted for the possible kinematical domains accessible in K_{e4}. As is obvious from the figure the s_ℓ dependence in this model is very linear and any curvature can be neglected within the expected experimental accuracy. The differences in the slope for the two values of s_π is small.

We now turn to the $\cos\theta_\pi$ dependence within this model. In Fig. 4 the form factors F and G are plotted for two values of s_π. For G it is extremely linear while for F a very small curvature is present. The latter is however below the expected experimental uncertainties and show that the effect of D-waves[2] is very small in this model. A linear best fit to F is also shown. The slope changes

[1] This will also be true in the next generation of experiments. We have in Fig. 14 shown the data of [1] with the points plotted at the average energy in the bins used.

[2] Meant is here and below, D waves for F and higher than D waves for G.

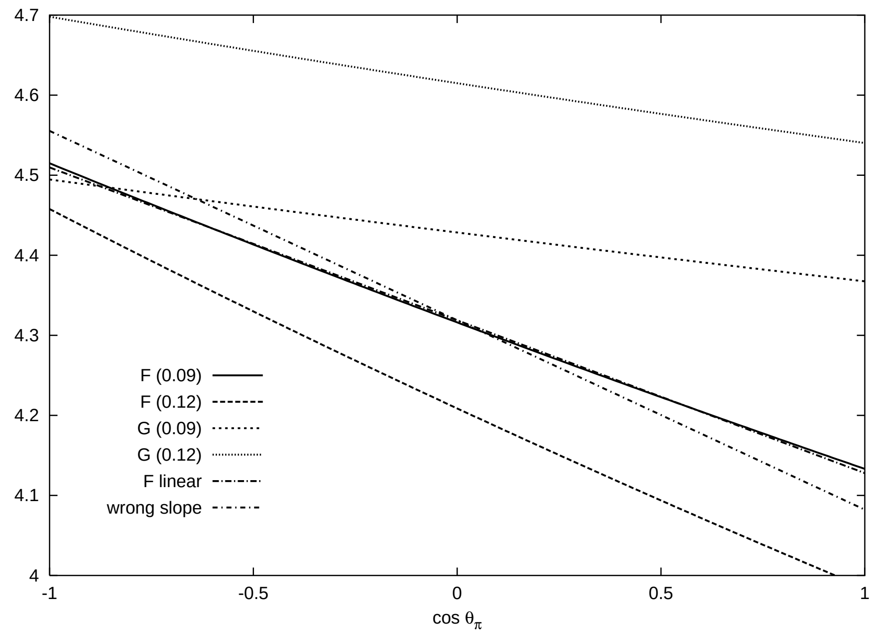

Figure 4: The form factor F and G of the model of Ref. [10] as a function of $\cos\theta_\pi$ at $s_\ell = 0$ and for $\sqrt{s_\pi} = 0.3$ GeV and $\sqrt{s_\pi} = 0.35$ GeV.

somewhat between the two values of $\sqrt{s_\pi}$. The linear best fits are :

$$
\begin{aligned}
F(\sqrt{s_\pi} = 0.3 \text{ GeV}) &= 4.319 - 0.191 \cos\theta_\pi \\
F(\sqrt{s_\pi} = 0.35 \text{ GeV}) &= 4.213 - 0.236 \cos\theta_\pi \\
G(\sqrt{s_\pi} = 0.3 \text{ GeV}) &= 4.429 - 0.064 \cos\theta_\pi \\
G(\sqrt{s_\pi} = 0.35 \text{ GeV}) &= 4.616 - 0.079 \cos\theta_\pi \qquad (4)
\end{aligned}
$$

The differences in the $\cos\theta_\pi$ part at the different energies are visible but do probably remain within the errors of the next generation of experiments. This can be seen in Fig. 4 where we have for F also plotted the linear fit with the slope of the curve at $\sqrt{s_\pi} = 0.35$ GeV with the central value of the curve at $\sqrt{s_\pi} = 0.3$ GeV. See also below for an approximate description of the s_π dependence.

So for this model a fit with linear s_π, a linear $\cos\theta_\pi$ and a linear s_ℓ dependence seems sufficient in the region where there will be accurate data.

4.2 Resonances using the model of Ref. [3]

Here we use the resonance parametrization as used in Ref. [3]. The difference with the previous section are that the resonances here only contribute at next-to-leading order in CHPT. We have therefore added the lowest order contribution $m_K/(\sqrt{(2)}F_\pi)$ to F and G in order to make the plots more comparable to the

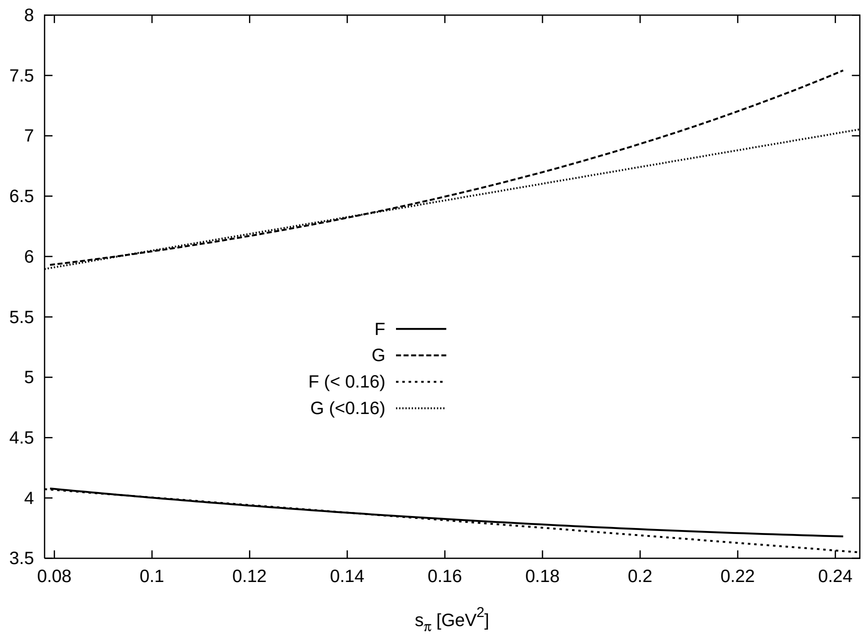

Figure 5: The form factor F and G of the model of Ref. [3] as a function of s_π at $\cos\theta_\pi = s_\ell = 0$.

previous section. In this parametrization there is also no contribution from the axial-vectors to K_{e4}, differences due to SU(3) breaking in the meson masses and couplings are also neglected but here scalars are included as well. In most cases however the main contribution comes from the vectors.

The conclusions are also the same as in the previous section even if there are some differences in the numerical estimates of the various coefficients involved.

In Fig. 5 we have shown the F and G form factors of this model as a function of s_π for $\cos\theta_\pi = s_\ell = 0$. In accordance with the discussion in Sect. 3 we see that there is again little curvature. The curvature visible in G is again due to the ρ-pole. We have checked this by setting $m_\rho = 1.37$ GeV in the model and then all curvature disappears. Experimentally there are very few events above $s_\pi = 0.16$ GeV^2 or $E_{\pi\pi} \leq 0.4$ GeV. In the figure the fits linear in s_π to the model curves below this energy are also shown. As can be seen the linear approximation is in the relevant region quite sufficient as an approximation to this model.

In Fig. 6 we plot the s_ℓ dependence of the form factors F and G for two values of s_π. The lines are only plotted for the possible kinematical domains accessible in K_{e4}. The s_ℓ dependence is very linear and any curvature can be neglected within the expected experimental accuracy. The differences in the slope for the two values of s_π is small.

We now turn to the $\cos\theta_\pi$ dependence within this model. In Fig. 7 the form factors F and G are plotted for two values of s_π. For G it is extremely linear

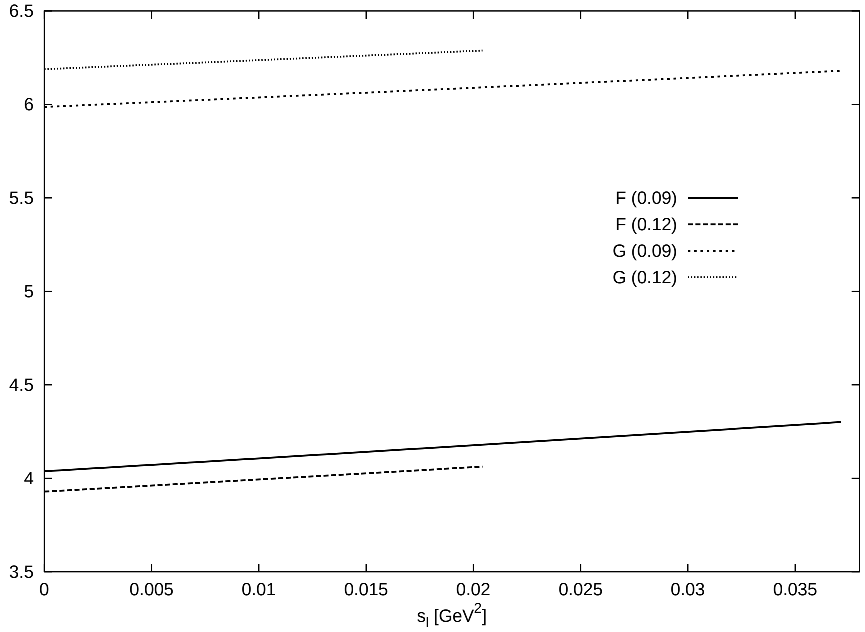

Figure 6: The form factor F and G of the model of Ref. [3] as a function of s_ℓ at $\cos\theta_\pi = 0$ and for $\sqrt{s_\pi} = 0.3$ GeV and $\sqrt{s_\pi} = 0.35$ GeV.

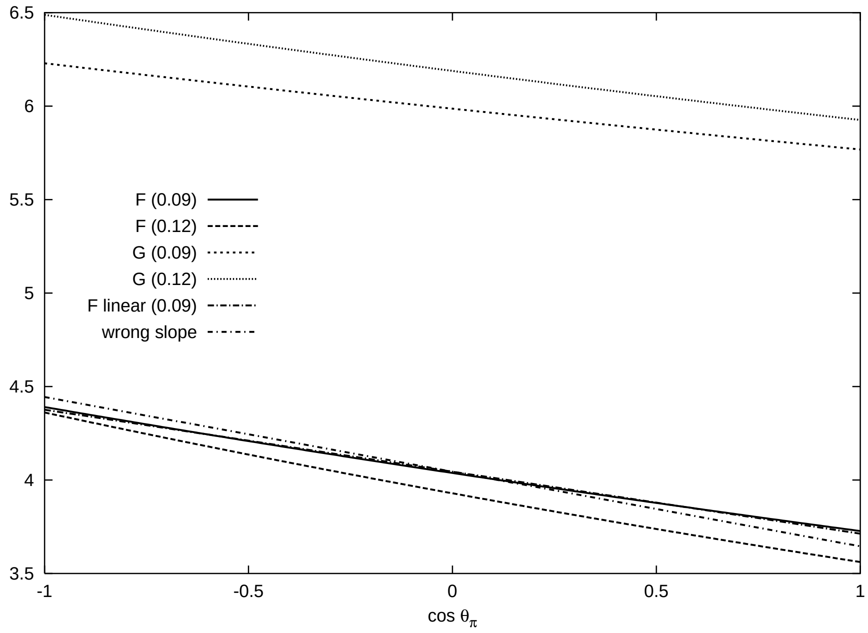

Figure 7: The form factor F and G of the model of Ref. [3] as a function of $\cos\theta_\pi$ at $s_\ell = 0$ and for $\sqrt{s_\pi} = 0.3$ GeV and $\sqrt{s_\pi} = 0.35$ GeV.

while for F a very small curvature is present. The latter is however below the expected experimental uncertainties and show that the effect of D-waves is very small in this model. A linear best fit to F is also shown. The slope changes somewhat between the two values of $\sqrt{s_\pi}$. The linear best fits are :

$$\begin{aligned}
F(\sqrt{s_\pi} = 0.3\ \mathrm{GeV}) &= 4.045 - 0.331\cos\theta_\pi \\
F(\sqrt{s_\pi} = 0.35\ \mathrm{GeV}) &= 3.940 - 0.399\cos\theta_\pi \\
G(\sqrt{s_\pi} = 0.3\ \mathrm{GeV}) &= 5.991 - 0.230\cos\theta_\pi \\
G(\sqrt{s_\pi} = 0.35\ \mathrm{GeV}) &= 6.195 - 0.281\cos\theta_\pi
\end{aligned} \tag{5}$$

The differences in the $\cos\theta_\pi$ part at the different energies are visible but do probably remain within the errors of the next generation of experiments.

So for this model again a fit with linear s_π, a linear $\cos\theta_\pi$ and a linear s_ℓ dependence seeme to be sufficient in the region where there will be accurate data.

5 One-loop CHPT

In Sect. 4 we discussed in two models the effects of the poles present in the various cuts. Now we switch to a discussion of the effects of the continuum. In this section we will use CHPT to order p^4. The contributions from the p^4 constants L_i to F and G are linear in the kinematical variables s_π, t and u thus all curvature present is from the loop diagrams. To one-loop these diagrams have possible two-particle cuts, the main ones are the $\pi\pi$ and the $K\pi$ ones as described in Sect. 3. Other cuts present in the loops are KK and $K\eta$. Their effect is however very linear in the kinematical variables. We use here the oneloop calculation of [4] in the notation of [3]. For definiteness we use the values of the L_i^r as given in the DAΦNE report[11] and all plots plot the real part only. Notice that this corresponds to the unitarized fit of Ref. [3] so the fact that the plots do not agree well with the data of [1] is due to the unitarization effects.

In Fig. 8 we have shown the F and G form factors of this model as a function of s_π for $\cos\theta_\pi = s_\ell = 0$. In accordance with the discussion in Sect. 3 we see that there is some curvature mainly generated by the $\pi\pi$ intermediate states. In the figure the fits linear in s_π to the model curves below $s_\pi = 0.16\ \mathrm{GeV}^2$ are also shown. As can be seen the linear approximation in the relevant region is sufficient within the precision of the present experiment [1]. It becomes somewhat borderline for the next generation of experiments but the situation improves somewhat if we fit $|F|$ instead of the real part of F. The effect of the latter we have checked in the unitarized case where the curvature is more pronounced.

Let us now turn to the s_ℓ dependence. In Fig. 9 the form factors F and G are plotted for two values of s_π. The lines are only plotted for the possible kinematical domains accessible in K_{e4}. As is obvious from the figure the s_ℓ dependence in

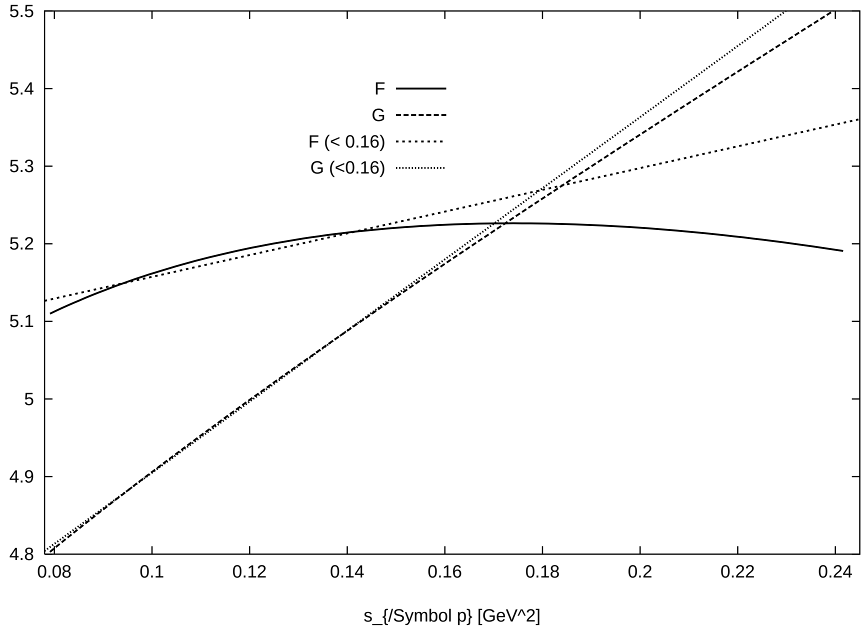

Figure 8: The form factor F and G in p^4 CHPT as a function of s_π at $\cos\theta_\pi = s_\ell = 0$.

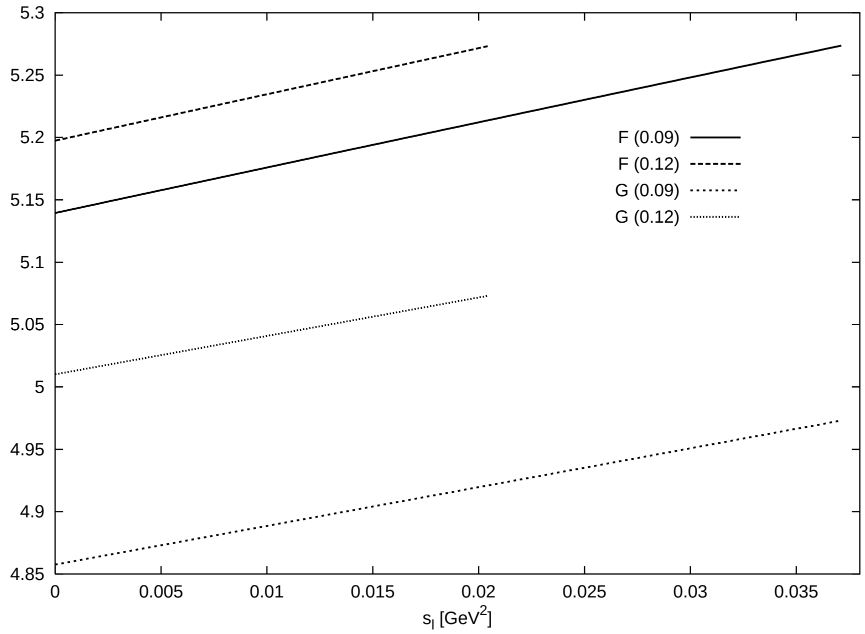

Figure 9: The form factor F and G in p^4 CHPT as a function of s_ℓ at $\cos\theta_\pi = 0$ and for $\sqrt{s_\pi} = 0.3$ GeV and $\sqrt{s_\pi} = 0.35$ GeV.

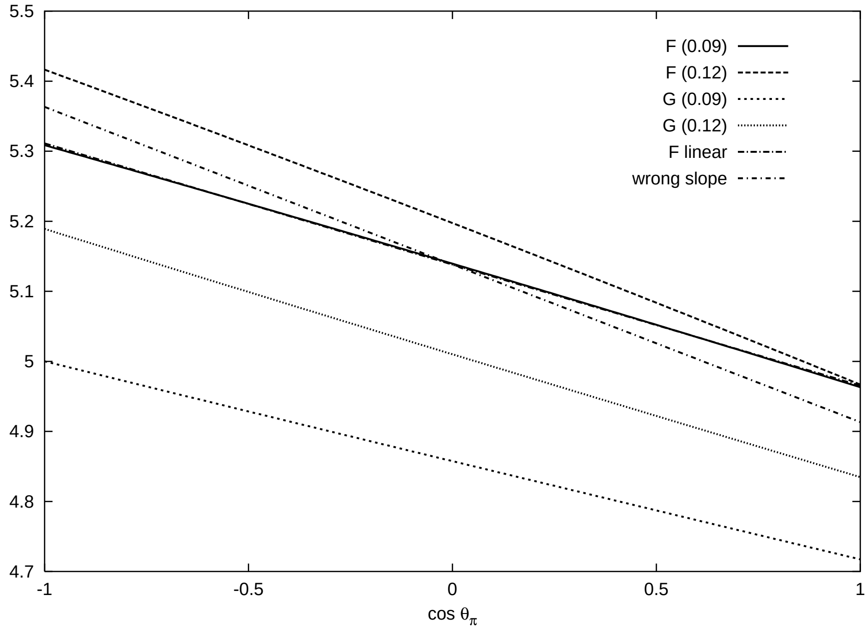

Figure 10: The form factor F and G in p^4 CHPT as a function of $\cos\theta_\pi$ at $s_\ell = 0$ and for $\sqrt{s_\pi} = 0.3$ GeV and $\sqrt{s_\pi} = 0.35$ GeV.

this model is again very linear and any curvature can be neglected within the expected experimental accuracy. The differences in the slope for the two values of s_π is small.

We now turn to the $\cos\theta_\pi$ dependence within p^4 CHPT. In Fig. 10 the form factors F and G are plotted for two values of s_π. For G it is extremely linear while for F a very small curvature is present. The latter is however below the expected experimental uncertainties and show that the effect of D-waves is very small. A linear best fit to F is also shown. The slope changes somewhat between the two values of $\sqrt{s_\pi}$. The linear best fits are :

$$\begin{aligned}
F(\sqrt{s_\pi} = 0.3 \text{ GeV}) &= 5.138 - 0.173\cos\theta_\pi \\
F(\sqrt{s_\pi} = 0.35 \text{ GeV}) &= 5.195 - 0.225\cos\theta_\pi \\
G(\sqrt{s_\pi} = 0.3 \text{ GeV}) &= 4.858 - 0.141\cos\theta_\pi \\
G(\sqrt{s_\pi} = 0.35 \text{ GeV}) &= 5.011 - 0.177\cos\theta_\pi \qquad (6)
\end{aligned}$$

The differences in the $\cos\theta_\pi$ part at the different energies are visible but do probably remain within the errors of the next generation of experiments.

At all relevant values of s_π the form factors are extremely linear in s_ℓ and $\cos\theta_\pi$. Parametrizing F as $F = f_s + f_p\cos\theta_\pi$ we get from one-loop CHPT $|f_p/f_s| = 0.043,\ 0.034,\ 0.008$ at $\sqrt{s_\pi} = 350,\ 300,\ 280$ MeV. This variation does probably stay within the future experimental errors. The curvature in s_π might

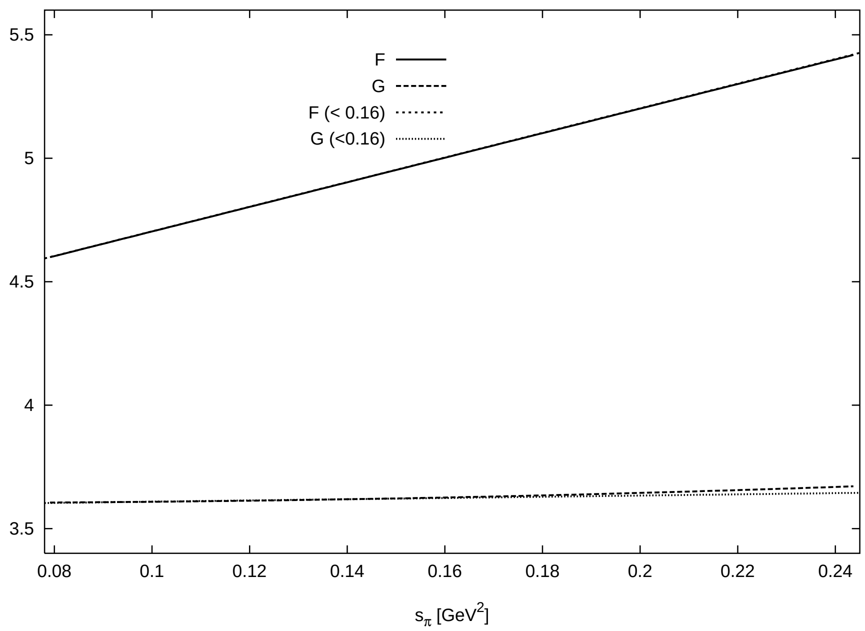

Figure 11: The form factor F and G in partial p^6 CHPT as a function of s_π at $\cos\theta_\pi = s_\ell = 0$.

become relevant in future experiments.

6 Double Logs

In this section we use the partial p^6 calculation of [12] for the F and G form factors. Here three types of contribution have been calculated using general renormalization methods. The relevant contributions are the ones proportional to $(\log(m_K^2/\mu^2))^2$, $L_i \log(m_K/\mu)$ and $L_i L_j$. The scale μ is the subtraction scale in CHPT and we have chosen the scale of the logarithms to be the Kaon mass. The reason for this is that the same approximation in the p^4 calculation gives a reasonable agreement with the full result for this choice. Figures 11 to 13 show the same plots as in the previous sections. We have plotted here the partial p^6 results with the lowest order added, the p^4 contribution is not included. The conclusions are basically the same as in the previous sections but notice that the curvature in F and G from this source is rather small. The contribution to the linear dependence on s_π, s_ℓ and $\cos\theta_\pi$ is typically smaller than the p^4 results but not negligible. Absolute numerical results from this section are quite dependent on the particular choices of input[12].

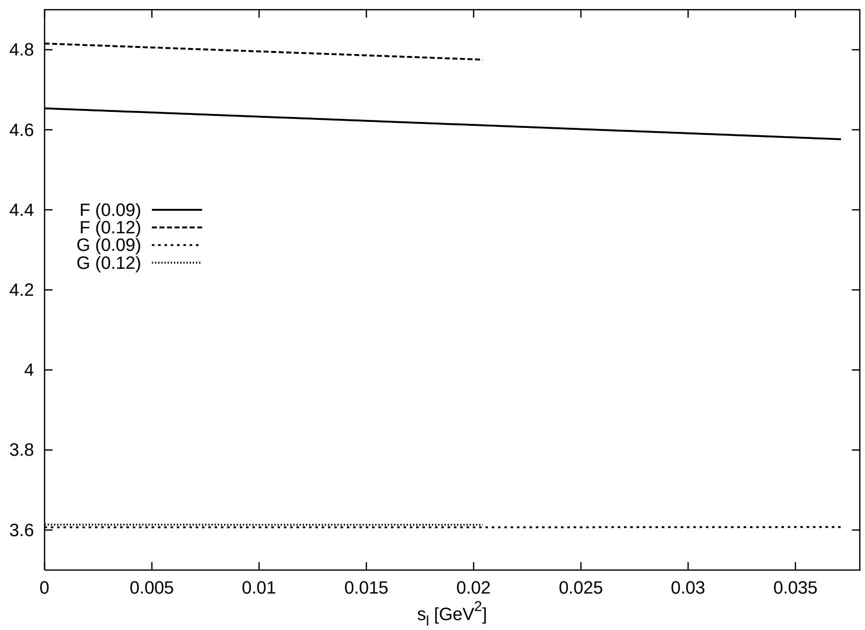

Figure 12: The form factor F and G in partial p^6 CHPT as a function of s_ℓ at $\cos\theta_\pi = 0$ and for $\sqrt{s_\pi} = 0.3$ GeV and $\sqrt{s_\pi} = 0.35$ GeV.

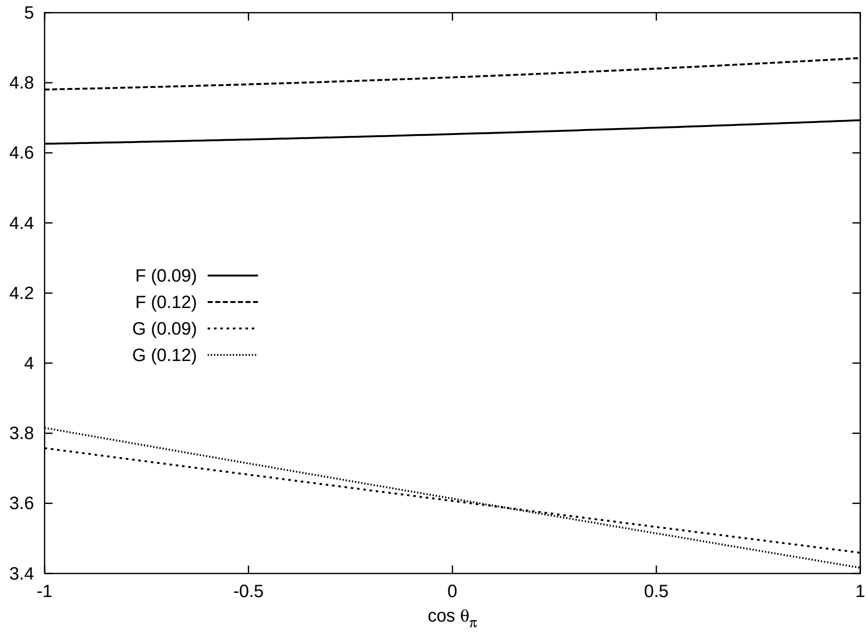

Figure 13: The form factor F and G in partial p^6 CHPT as a function of $\cos\theta_\pi$ at $s_\ell = 0$ and for $\sqrt{s_\pi} = 0.3$ GeV and $\sqrt{s_\pi} = 0.35$ GeV.

7 Unitarization of F

As we have seen in the plots, the behaviour of the form factors are almost linear in the models. Also, as we expected, the contribution from the S-wave from the $\pi\pi$ scattering produces some curvature in the F form factor that becames more clear in the case of the one-loop ChPT result. We will now discuss the S-wave part of this form factor, which is the source of the curvature using the unitarization method [13, 14]. It consists in writing a dispersive relation for the partial wave using the ChPT limit to fix the subtraction constants. A previous study of the analytic properties separating the regions $s_\pi < 0$ and $s_\pi > 0$ provided a good way to introduce a general parametrization for the S-wave [15], and the contribution from resonances in the t-channel (see [3] for details).

The result is shown in Fig. 14. The curve $|f|_{NR}$ represents the absolute value for the S-wave, where the contribution from the resonance sector, and therefore from the $s_\pi < 0$ region, is null. The other curves are the real and absolute value for the case with resonances. We have shown here both the absolute value and the real part for one case to show that the absolute value is more linear. The latter is the relevant one for fitting to the experimental data.

A linear fit to the relevant energies for s_π is also plotted. The importance of the rescattering effects in the S-wave is obvious, not only because of the modification of the linear behaviour, that can be explained by the fact that the cut is in the physical region, but also because of the contribution from the imaginary part.

8 The H form factor

The previous sections were devoted to the form factors F and G related to the cuts (b), (c) and (d) of the Fig. 1. It remains to discuss the behaviour related to the H form factor. Using the 1-loop ChPT result, which is here order p^6, and the hypothesis of resonance saturation for the unknown $O(p^6)$ constants, the behaviour of this form factor is not only linear but constant around the experimental value $H(s_\pi = 0) = -2.68 \pm 0.68$ [1]. There is a cancellation among the different contributions such that in the final curve the dependence with the energy is not appreciable, and the correction to the leading order is small [8]. Looking at the dependence with s_ℓ and $\cos\theta_\pi$ the shape is basically not modified with respect to the constant value.

9 A sufficient parametrization

In all the models/approximations analyzed in the previous sections we observed that F and G were always very linear in s_ℓ with a slope that was very similar for both values of s_π. We also observed that F and G were very linear in $\cos\theta_\pi$ but with slopes somewhat varying between the two energies. The form factors

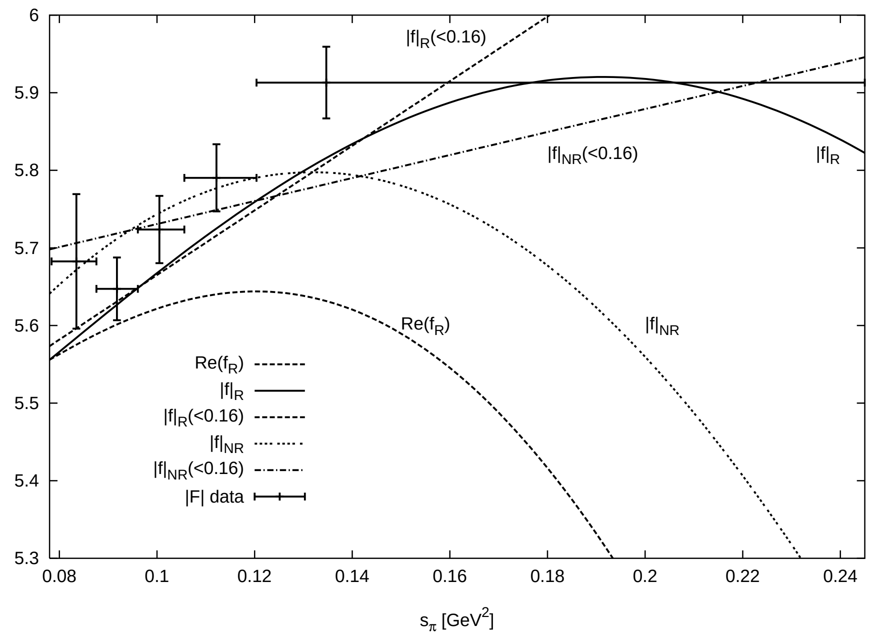

Figure 14: The S-wave in F using unitarization with (f_R) and without (f_{NR}) resonances as a function of s_π at $s_\ell = 0$. The linearized fits for $\sqrt{s_\pi} < 0.16$ GeV are also plotted.

depend on s_π, t and u and the effects of the singularities other than the $\pi\pi$ ones can be expanded in t and u. By expanding to first order in these quantities we then indeed observe that both F and G have the structure

$$W = w(s_\pi) + w_1 s_\ell + w_2 \sigma_\pi X \cos\theta_\pi \,. \tag{7}$$

Where we used $t - u = -2\,\sigma_\pi\ X\ \cos\theta_\pi$ with

$$\sigma_\pi = \sqrt{1 - \frac{4m_\pi^2}{s_\pi}}, \quad X = \frac{1}{2}\lambda^{1/2}(m_K^2, s_\pi, s_\ell)\,, \quad \lambda(a,b,c) = (a-b-c)^2 - 4bc\,. \tag{8}$$

Checking Eqs. (4),(5) and (6) we see that the s_π dependence of the coefficient of $\cos\theta$ is indeed well described by $\sigma_\pi X$.

Using the partial wave expansions and their respective phases δ_ℓ^I (I: isospin, ℓ: angular momentum), we then obtain as a parametrization [3]

$$\begin{aligned} F &= (f_s(s_\pi) + f_1\, s_\ell)e^{i\delta_0^0(s_\pi)} + \tilde{f}_p\, \sigma_\pi X \cos\theta_\pi e^{i\delta_1^1(s_\pi)} \\ G &= (g_p(s_\pi) + g_1\, s_\ell)e^{i\delta_1^1(s_\pi)} + g_d\, \sigma_\pi X \cos\theta_\pi e^{i\delta_2^0} \end{aligned} \tag{9}$$

[3] $\tilde{f}_p$ is a combination of the standard f_p and g_p partial waves

Then the curvature in s_π in G is mainly due to the ρ resonance and in the experimentally relevant region is rather well described by a linear function in s_π. We therefore advocate the use of

$$G = \left(g_p + g_p'\, s_\pi + g_\ell\, s_\ell\right) e^{i\delta_1^1(s_\pi)} + g_d\, \sigma_\pi X \cos\theta_\pi e^{i\delta_2^0(s_\pi)} \tag{10}$$

The phase δ_1^1 is relatively small and the last term in G is already a small correction so one can neglect the difference between δ_1^1 and δ_2^0 as well. For $f_s(s_\pi)$ a linear approximation will be somewhat borderline, inclusion of a quadratic term is therefore useful and its presence should be checked in the data:

$$f_s(s_\pi) = f_s + f_s' s_\pi + f_s'' s_\pi^2\,. \tag{11}$$

For H a linear approximation in s_π should be sufficient

$$H = \left(h_p + h_p'\, s_\pi\right) e^{i\delta_1^1(s_\pi)}\,. \tag{12}$$

So within this approximation we have 11 parameters plus the number of bins in s_π for $(\delta_0^0 - \delta_1^1)(s_\pi)$ as fitting parameters.

10 Conclusions

We presented the results from several models for the form factors F and G and of CHPT calculations and extensions. We have shown that a simple linear parametrization of the dependence on the kinematical variables is sufficient in most of the region where there will be sufficient data with the possible exception of the S-wave part of the F form-factor. Even there a linear fit is quite a good approximation but then care has to be taken to define the theoretical slope.

We showed that 11 parameters in addition to the phases are quite sufficient to fit the expected accuracy of the experiment and this should allow to determine those phases more accurately as a function of s_π compared to the case where everything is fitted on a bin-by-bin basis.

11 Acknowledgements

We thank Juerg Gasser, Bachir Moussallam and Stefan Pislak for useful comments.

References

[1] L. Rosselet et al., Phys. Rev. D15 (1977) 574.

[2] J. Bijnens et al., hep-ph/9411311, chapter 7.1 in “The Second DAΦNE PHYSICS HANDBOOK”, eds. L. Maiani, G. Pancheri and N. Paver, INFN, Frascati.

[3] J. Bijnens, G. Colangelo and J. Gasser, Nucl. Phys. B427 (1994) 427 (hep-ph/9403390).

[4] J. Bijnens, Nucl. Phys. B337 (1990) 635;
C. Riggenbach et al., Phys. Rev. D43 (1991) 127.

[5] L.-M. Chounet, J.-M. Gaillard and M.K. Gaillard, Phys. Rep. C4 (1972) 199.

[6] A. Pais and S.B. Treiman, Phys. Rev. 168 (1968) 1858.

[7] G. Colangelo, M. Knecht and J. Stern, Phys.Lett. B336 (1994) 543 (hep-ph/9406211).

[8] Ll. Amettler et al., Phys. Lett. B303 (1993) 140.

[9] G. Ecker et al., Nucl. Phys. B321 (1989) 311.

[10] M. Finkemeier and E. Mirkes, Z. Phys. C69 (1996) 243 (hep-ph/9503474).

[11] J. Bijnens, G. Ecker and J. Gasser, hep-ph/9411232, chapter 3 in “The Second DAΦNE PHYSICS HANDBOOK”, eds. L. Maiani, G. Pancheri and N. Paver, INFN, Frascati.

[12] J. Bijnens, G. Colangelo and G. Ecker, Phys. lett. B441 (1998) 437 (hep-ph/9808421).

[13] J. Donoghue, J. Gasser and H. Leutwyler, Nucl. Phys. B343 (1990) 341.

[14] A.D. Martin and T.D. Spearman, Elementary particle theory (North-Holland, Amsterdam, 1970).

[15] A. Schenk, Nucl. Phys. B363 (1991) 97.